임상의과학석사 학위논문

소아의 경부 림프절 비대: 초음파 소견 및 임상 소견에 근거한 진단나무모형

Cervical lymphadenopathy in Children: a diagnostic tree analysis model based on US and clinical findings

2019 년 10 월

서울대학교 대학원

임상의과학과 석사 과정

박지은

Abstract

Cervical lymphadenopathy in Children: a diagnostic tree analysis model based on ultrasonographic and clinical findings

Ji Eun Park

Collage of Medicine, Department of Clinical Medical Sciences
The Graduate School
Seoul National University

Purpose: To establish a diagnostic tree analysis (DTA) model based on ultrasonography (US) findings and clinical characteristics for differential diagnosis of common cervical lymphadenopathy in children.

Materials and Methods: A total of 242 patients (131 boys, 111 girls; mean age, 11.2±0.3 years; range, 1 month to 18 years) with pathologically confirmed Kikuchi disease (n=127), reactive hyperplasia (n=64), lymphoma (n=24), or suppurative lymphadenitis (n=27) who underwent neck US were included. US images were retrospectively reviewed to assess lymph node (LN) characteristics and clinical information was collected from patient records. DTA models were created using a classification and regression tree algorithm on the basis of US imaging and clinical

findings. The patients were randomly divided into training (70%, 170/242) and validation (30%, 72/242) datasets to assess the diagnostic performance of the DTA models.

Results: In the DTA model based on all predictors, perinodal fat hyperechogenicity, LN echogenicity, and short diameter of the largest LN were significant predictors for differential diagnosis of cervical lymphadenopathy (overall accuracy, 85.3% and 83.3% in the training and validation datasets, respectively). In the model based on categorical parameters alone, perinodal fat hyperechogenicity, LN echogenicity, and loss of fatty hilum were significant predictors (overall accuracy, 84.7% and 86.1% in the training and validation datasets, respectively).

Conclusions: Perinodal fat hyperechogenicity, heterogeneous echotexture, short diameter of the largest LN, and loss of fatty hilum were significant US findings in the DTA for differential diagnosis of cervical lymphadenopathy in children. However, the application of short-diameter cutoff values is limited by population diversity, and other clinical and radiological findings should be taken into account.

Keywords: Lymphadenopathy, Ultrasonography, Decision trees, Kikuchi disease, Lymphoma

Student Number: 2018-24517

Table of contents

I. Introduction ·····1

II. Materials and methods

A. Patient Selection ·····4

B. Ultrasonography, core needle biopsy and fine needle aspiration ·····5

C. Image Analysis ·····6

D. Statistical Analysis ·····8

III. Results

A. Clinical characteristic ·····11

B. Neck US imaging findings ·····12

C. DTA Models ·····14

D. External Validation of the Diagnostic Tree·····15

IV. Discussion ·····17

V. Reference ·····24

VI. Abstract (in Korean) ·····41

List of tables

Table 1. Comparison of Clinical Characteristics for Kikuchi Disease, Reactive Hyperplasia, Lymphoma, and Suppurative Lymphadenitis ·····30

Table 2. Comparison of Neck US Imaging Findings for Kikuchi Disease, Reactive Hyperplasia, Lymphoma, and Suppurative Lymphadenitis ·····32

Table 3. Performance of the Diagnostic Trees ·····35

List of figures

Figure 1. Flowchart for patient inclusion ·····36

Figure 2 a–d. Representative ultrasonographic images in patients with Kikuchi's disease, reactive hyperplasia, lymphoma, and suppurative lymphadenitis ·····37

Figure 3. Diagnostic tree derived from all predictors of imaging findings and clinical information ·····39

Figure 4. Diagnostic tree derived from categorical predictors of imaging findings and clinical information ·····40

Introduction

Cervical lymphadenopathy is one of the most common problems encountered in children [1]. Since cervical lymphadenopathy is a non-specific clinical manifestation of various diseases, its differential diagnosis should cover a wide range of diseases. Although patient history and physical examination provide substantial information, further work-up to identify the underlying etiology is required in many cases [2-6].

Although infectious lymphadenitis is the major etiology of pediatric cervical lymphadenopathy, various noninfectious causes also require diagnostic consideration, including malignancies such as lymphoma, and inflammatory lymphadenitis such as Kikuchi's disease, Kawasaki disease, and connective tissue disorders-associated lymphadenopathies. The diagnostic work-up or therapeutic strategy varies significantly according to the underlying diseases of suspicion. For instance, in cases suggestive of lymphoma, core needle biopsy (CNB) or excisional biopsy is essential for diagnosis, whereas in cases suggestive of Kikuchi disease, which generally has a self-limiting benign course, biopsy may not be necessary. However, Kikuchi disease can initially mimic

the clinical presentation of lymphoma, as it generally presents with fever, cervical lymphadenopathy, and night sweats [7–8]; therefore, a biopsy is occasionally performed in these cases for differentiation. Moreover, even cases of clinically suspected lymphadenopathy associated with Kikuchi disease or infectious lymphadenitis often require further diagnostic assessments, such as image examinations or biopsy, to rule out malignancy or rare diseases. Thus, appropriate establishment of a presumptive diagnosis based on clinical information and imaging findings is crucial for determining the further diagnostic work-up [9].

Ultrasonography (US) is the most appropriate imaging modality for initial assessment of pediatric cervical lymphadenopathy because of its availability and non-invasiveness [10]. Unlike computed tomography (CT), US does not involve radiation exposure, contrast media, or sedatives. Moreover, US provides high-resolution imaging information of LN characteristics, including size, shape, margin, internal echogenicity, vascularity, and perinodal soft tissue.

Although multiple diseases should be comprehensively considered as the etiology of cervical lymphadenopathy in children,

most studies on US imaging findings of pediatric cervical lymphadenopathy only cover two diseases of interest, such as metastasis vs. reactive lymphadenopathy, Kawasaki disease vs. lymphadenitis, tuberculous lymphadenitis vs. Kikuchi disease, and lymphatic disease vs. metastatic disease [11–14]. According to previous studies, a combination of multiple imaging features instead of a single imaging finding has been found to be useful in discriminating causes in cervical lymphadenopathy among children [13; 15–17]. Therefore, assessment of pediatric lymphadenopathy requires a method of discriminating various diseases by combining various clinical and imaging findings, that is, a diagnostic tree analysis (DTA) model. Although the diagnostic tree for necrotic cervical lymphadenopathy in adults has been published [18], there are no corresponding studies on children. Thus, our study aimed to suggest a DTA model based on US findings and clinical characteristics for differential diagnosis of common cervical lymphadenopathy in children.

Material and methods

Patients selection

Patients under 19 years of age who underwent neck US with pathologic confirmation of the lymphadenopathy from 2012 to 2018 (n = 927) were included in our study. Among these patients, 316 received pathologic confirmation of the enlarged cervical LN (CNB, 230; fine needle aspiration [FNA], 44; and excisional biopsy [with or without CNB or FNA], 42). Our study intended to establish a DTA model based on imaging findings and clinical characteristics for differential diagnosis of common cervical lymphadenopathy in children; therefore, we excluded 74 patients due to the following reasons: (a) disease groups with less than twenty patients (n = 35) and (b) inconclusive pathologic results (n = 39). Since FNA yielded many inconclusive reports, including "nonspecific benign" or "inadequate," diagnoses by FNA results were accepted as definitive diagnoses only in the suppurative lymphadenitis group or lymphoma group. The flowchart for patient inclusion is shown in Fig. 1.

Finally, a total of 242 patients (131 boys and 111 girls; mean age, 11.2 ± 0.3 years; range, 1 month to 18 years) with

pathologically confirmed Kikuchi disease (n = 127), reactive hyperplasia (n = 64), lymphoma (n = 24), and suppurative lymphadenitis (n = 27) who underwent neck US were included. The patients underwent FNA (n = 15), CNB (n = 195), or excisional biopsy (n = 32) for histopathological confirmation.

Clinical information was reviewed, including age, sex, cervical tenderness, erythema, heat sense, fever, hepatomegaly, splenomegaly, and history of antibiotic use. In addition, laboratory results such as white blood cell (WBC) count, C-reactive protein (CRP) level, and erythrocyte sedimentation rate (ESR) were collected.

Ultrasonography, core needle biopsy, and fine needle aspiration

Grayscale and color Doppler US images were obtained with a Philips ultrasonography system (iU22 or EPIQ 7G; Philips Healthcare, Bothell, WA, USA) equipped with a linear high-frequency transducer (5–12 MHz or 5–18MHz). Color Doppler ultrasound was acquired only when the patient was cooperative

(195/242 patients, 80.6%).

Two experienced pediatric radiologists (J.Y.K. and Y.J.R., with 14 and 8 years of clinical experience, respectively) performed US-guided CNB on the most representative node by using a disposable 18-gauge gun biopsy needle (TSK Ace-cut; Create Medic, Yokohama, Japan or Stericut with a coaxial guide, TSK Stericut; TSK Laboratory, Soja, Japan). After local anesthesia with 1% lidocaine, the cortex of the LN was obtained using a biopsy needle. In cases with suppurative lymphadenitis, US-guided FNA was performed using 18- or 20-gauge needles (Angiocath; Becton Dickinson Infusion therapy Systems, Sandy, UT) on the necrotic LN after local anesthesia. The need for sedation was determined according to the patient's cooperation.

Image analysis

US images of LNs were retrospectively reviewed using picture archival and communication system (PACS). Imaging analysis was performed by two radiologists (Y.J.R. and J.E.P with 8 years and 4 years of clinical experience, respectively) independently. The

reviewers were blinded to the clinical history and the pathologic diagnosis of the lymphadenopathy.

For whole US images, the laterality of the lymphadenopathy (unilateral vs. bilateral), presence of posterior neck involvement, number of involved LNs (single vs. several vs. multiple), regional distribution (conglomerated vs. multiple separated), and size distribution (even vs. uneven) were assessed. Among the enlarged LNs, the largest LN was selected as the representative LN. However, for LNs with abnormal imaging findings, the largest LN with abnormal features was the representative LN. The authors measured the long diameter (LD) and short diameter (SD) of the largest cervical LN in the axial image, and the SD/LD ratio was calculated. In addition, echogenicity of the LN in comparison with the adjacent neck muscle, heterogeneity of the echogenicity, margins, presence of necrosis or abscess, calcification, loss of normal fatty hilum, perinodal fluid dispersion, and perinodal fat hyperechogenicity were evaluated for the representative LN. In color Doppler US images of a representative LN, LN hilar vascularity and perinodal or cortical vascularity were analyzed.

Statistical analysis

Statistical analysis was performed using open-source statistical software R, version 3.4.2 (http://www.R-project.org) and SPSS, version 22 (SPSS Inc, Chicago, Ill). All clinical and radiological variables were compared in the four groups (Kikuchi disease, reactive hyperplasia, lymphoma, and suppurative lymphadenitis). In all of the tests, p-values less than 0.05 were considered statistically significant. Pearson's chi-squared test or Fisher's exact test were used to compare categorical variables among the groups. Kruskal-Wallis rank sum test or one-way ANOVA were performed in continuous variables.

Interclass correlation coefficient and weighted kappa were used for assessing inter-reader reliability in continuous and categorical variables. Weighted kappa values of 0–0.20 (poor), 0.21–0.40 (fair), 0.41–0.60 (moderate), 0.61–0.80 (good), and 0.81–1.00 (very good) and interclass correlation coefficient values of 0–0.20 (poor), 0.21–0.40 (fair), 0.41–0.60 (moderate), 0.61–0.80 (strong), and 0.81–1.00 (excellent) were obtained.

To create a DTA model for differential diagnosis of cervical

lymphadenopathy in children, a classification and regression tree (CART) algorithm was used (minimum cases in the parent node, 20; minimum cases in the child node, 20; maximum tree depth, 30). The following clinical and US findings were used to establish the DTA model: (a) clinical findings: age, sex, cervical tenderness, erythema, heat sense, fever, prolonged fever (>2 weeks), hepatomegaly, splenomegaly, history of antibiotic use, and laboratory results (WBC, ERC, and CRP), (b) US findings: laterality, posterior neck involvement, number, regional distribution, size distribution, nodal level, LD, SD echogenicity compared with adjacent neck muscle, heterogeneity of the echogenicity, margins, presence of necrosis or abscess, calcification, loss of fatty hilum, perinodal fluid collection, perinodal fat hyperechogenicity, LN hilar vascularity, and perinodal/cortical vascularity. Two different predictor variable sets were used: 1, all predictors mentioned above; 2, categorical predictors alone. Among the continuous variables, the SD of the largest LN, WBC count, and LN shape were converted to nominal variables for the second DTA model (short diameter of the largest LN: subcentimeter [SD < 10 mm] or others [SD ≥ 10 mm]; WBC: leukopenia [WBC < 4 × 103], normal range [4 × 103 ≤ WBC < 12 ×

103], or leukocytosis [WBC ≥ 12 × 103]; LN shape: elongated [SD/LD ratio < 0.5], oval [0.5 ≤ SD/LD ratio < 0.7], or round [SD/LD ratio ≥ 0.7]).

Each disease group was randomly divided into training (70%, total 170/242 [Kikuchi disease: 89, reactive hyperplasia: 45, lymphoma: 17, suppurative lymphadenitis: 19]) and validation (30%, total 72/242 [Kikuchi disease: 38, reactive hyperplasia: 19, lymphoma: 7, suppurative lymphadenitis: 8]) datasets to assess the diagnostic performance of the DTA model. The accuracy of the diagnostic tree was calculated and validated using the external validation dataset.

Results

Clinical characteristics

A comparison of the clinical characteristics among the four disease groups is shown in Table 1. There were 131 boys and 111 girls. The mean age of the patients was 11.17 ± 0.31 years (range, 1 month to 18 years).

Cervical tenderness was the most common clinical presentation in suppurative lymphadenitis (77.8%, 21/27). None of the lymphoma patients showed cervical erythema or cervical heat sense. Fever was frequently presented in Kikuchi disease (73.2%, 93/127) and suppurative lymphadenitis (70.4%, 19/27). Few patients had hepatomegaly (1.2%, 3/242) or splenomegaly (2.1%, 5/242).

Most patients underwent assessment of serum ESR (erythrocyte sedimentation rate) and CRP (C-reactive protein) levels, and these levels were the highest in suppurative lymphadenitis (ESR: 40.21 ± 31.05, CRP: 3.52 ± 3.46). Among the patients with Kikuchi disease, leukopenia was the most common finding in WBC counts (61.9%, 73/127). WBC counts were mostly in the normal range in reactive hyperplasia (70.0%, 35/64) and lymphoma (79.2%, 19/24). The

majority of suppurative lymphadenitis patients had leukocytosis (63.0%, 17/27).

Neck US imaging findings

Table 2 summarizes the US imaging findings in the four disease groups. In Kikuchi disease and suppurative lymphadenitis, lymphadenopathy was usually unilateral (74.8%, 95/127; 96.3%, 26/27, respectively). However, posterior neck involvement was common in Kikuchi disease (73.2%, 93/127) while it was rare in suppurative lymphadenitis (7.4%, 2/27). Multiple lymphadenopathy and conglomerated distribution were the most common in Kikuchi disease (91.3%, 116/127; 89.8%, 114/127). The size of the enlarged LNs showed a relatively even distribution in Kikuchi disease (83.5%, 106/127), while the other three disease groups showed uneven distributions.

The mean SDs of the largest LN in lymphoma and suppurative lymphadenitis were greater than those in Kikuchi disease and reactive hyperplasia. Most cases of lymphoma and suppurative lymphadenitis showed SDs greater than 10 mm, whereas most

cases of Kikuchi disease and reactive hyperplasia showed SDs less than 10 mm (Kikuchi disease, 8.56 ± 2.95 mm; reactive hyperplasia, 8.28 ± 3.23 mm; lymphoma, 17.27 ± 7.64 mm; and suppurative lymphadenitis, 18.43 ± 6.00 mm).

Representative LNs were usually homogeneous in Kikuchi disease (100.0%, 127/127) and reactive hyperplasia (92.2%, 59/64) whereas they usually exhibited heterogeneous echogenicity in suppurative lymphadenitis (96.3%, 26/27) and lymphoma (58.3%, 14/24). In suppurative lymphadenitis, enlarged LNs were generally ill-defined (85.2%, 23/27) and intranodal necrosis or abscess (85.2%, 23/27) were common, while the other three disease groups showed well-defined margins with little or no intranodal necrosis or abscess.

Most cases of Kikuchi disease (92.1%, 117/127) and suppurative lymphadenitis (96.3%, 26/27) demonstrated perinodal fat hyperechogenicity while lymphoma and reactive hyperplasia did not. Loss of fatty hilum was more common in lymphoma (70.8%, 17/24) and suppurative lymphadenitis (88.9%, 24/27) than in Kikuchi disease (0.8%, 1/127) and reactive hyperplasia (3.1%, 2/64). There was no LN calcification in all US examinations of the

four diseases.

Most patients in the four disease groups also underwent color Doppler US examinations (Kikuchi disease: 81.1%, 103/127; reactive hyperplasia: 76.6%, 49/64; lymphoma: 87.5%, 21/24; and suppurative lymphadenitis: 81.48%, 22/27). Color Doppler examinations of LNs in suppurative lymphadenitis (86.4%, 19/22) and lymphoma (66.7%, 14/22) showed more frequent abnormal hilar vascularity while most LNs in Kikuchi disease (99.0%, 102/103) and reactive hyperplasia (93.9%, 46/49) had normal hilar vascularity.

The representative cases of the four disease groups are presented in Fig. 2. Interobserver agreement of the imaging findings was good or excellent (0.743–0.991).

DTA Models

The summary of the two DTA models derived from all predictors and categorical predictors alone is shown in Figs. 3 and 4. The accuracies of the diagnostic trees in the training and validation

datasets are shown in Table 3.

In the DTA model based on all predictors, perinodal fat hyperechogenicity, LN echogenicity, and SD of the largest LN were found to be significant predictors in the diagnostic algorithm for differential diagnosis of cervical lymphadenopathy. The overall accuracy with 95% confidence interval (CI) was 85.3% (79.1%–90.3%). In contrast, in the DTA model based on categorical parameters alone, perinodal fat hyperechogenicity, LN echogenicity, and loss of fatty hilum were significant predictors. The overall accuracy with 95% CI was 84.7% (78.4%–89.8%), which was similar to that of the model from all predictors. In contrast, none of the clinical variables was a statistically significant predictor in both models.

External validation of the diagnostic tree

The overall accuracies of the external validation dataset with 95% CI were 83.3% (72.7%–91.1%) and 86.1% (75.94%–93.1%) based on all predictors and categorical predictors alone, respectively. The validation datasets consisted of a total of 72 patients (38 boys and

34 girls; mean age, 10.6 ± 5.25 years; range, 1 month to 18 years).

Discussion

For differential diagnosis of cervical lymphadenopathy in children, perinodal fat hyperechogenicity, LN echogenicity, SD of the largest LN, and loss of fatty hilum were significant predictors in our study. The DTA derived from all clinical and radiologic findings showed an accuracy of 85.3% in the training dataset and 83.3% in the external validation dataset to distinguish four diseases, namely, Kikuchi disease, reactive hyperplasia, lymphoma, and suppurative lymphadenitis. In this analysis, the significant predictors were perinodal fat hyperechogenicity, LN echogenicity, and SD of the largest LN. For the dataset using only nominal variables, accuracy was reported to be 84.7% in the training dataset and 86.1% in the external validation dataset. In this diagnostic tree, significant predictors were perinodal fat hyperechogenicity, LN echogenicity, and loss of fatty hilum.

In this study, the presence of perinodal fat hyperechogenicity was a key predictor to differentiate Kikuchi disease and suppurative lymphadenitis from lymphoma and reactive hyperplasia. Several reports have described perinodal infiltrations in Kikuchi disease [18–22] and suppurative lymphadenitis [23]. Likewise, perinodal

fat hyperechogenicity, which appears as a peripheral halo or periadenitis, is a common feature of Kikuchi disease (92.1%, 117/127) and suppurative lymphadenitis (96.3%, 26/27) in this study. The mechanism underlying perinodal fat hyperechogenicity is explained by inflammatory capsular destruction of the LN and perinodal infiltration of the lymphoid cells, histiocytes, and especially in Kikuchi disease, karyorrhectic debris (fragmentation of nuclei of dying cells and chromatin) [13; 18; 24–26]. However, perinodal fat hyperechogenicity could be detected in lymphoma or metastasis due to extracapsular extension of the disease, which implies the possibility of misclassification in the DTA.

Heterogeneity of the internal echotexture of LN is a unique factor in suppurative lymphadenitis that can help distinguish it from Kikuchi disease. In Kikuchi disease, all LNs (100.0%, 127/127) showed homogeneous echotexture and none showed intranodal necrosis. On the other hand, most cases of suppurative lymphadenitis demonstrated heterogeneous echotexture (96.3%, 26/27), frequently accompanied by LN necrosis or perinodal abscess formation (85.2%, 23/27). Heterogeneous echotexture and intranodal necrosis are caused by pyogenic organisms such as

Staphylococcus aureus or Streptococcus pyogenes that can cause acute inflammatory reactions, and recruitment of neutrophils may result in gross abscess formation composed of non-cellular materials [27-29]. In contrast, intranodal necrosis of Kikuchi disease is a microscopic necrosis demonstrated only on contrast-enhanced CT or MRI, not on US. Internal necrosis in Kikuchi disease is a coagulative necrosis that is composed of various cellular materials such as eosinophilic fibrinoid deposits, karyorrhectic debris, histiocytes, and immunoblasts [21; 25; 30; 31]. Moreover, radiologic examinations are usually performed in the early proliferative stage of Kikuchi disease before the necrosis is not formed [32]. Thus, the necrosis in Kikuchi disease on US is rarely observed, in contrast to suppurative lymphadenitis, and is also indistinguishable from the non-necrotic solid portions.

Loss of fatty hilum was a useful feature for differentiating lymphoma from reactive hyperplasia when perinodal fat hyperechogenicity was absent. In this study, 96.9% (62/64) of the reactive hyperplasia patients showed normal fatty hilum of the LN, while 70.8% (17/24) of lymphoma patients demonstrated absence of hilum. Several studies [33-36] have reported that loss of

echogenic hilum may found in malignancy, and according to Leboulleux et al. (2007) [37], in follow-up of thyroid cancer patients, preservation of a fatty hilum was a major criteria that excludes malignancy, showing 100% sensitivity. In malignant diseases such as lymphoma and metastasis, loss of hilum, nodal internal heterogeneity, and irregular nodal contour are the characteristic features in US [38].

With regard to size, LNs are generally considered to be in the normal range if their SD is less than 1 cm [39]. However, some studies suggested different size criteria depending on the location of the LN [40; 41], and there are few studies describing specific diagnoses of lymphadenopathy by size. According to Slap et al. [42], among children and young adults who underwent biopsy for peripheral lymphadenopathy, LNs greater than 2 cm were associated with granuloma or malignancy. However, when we converted the SD of the largest LN into a nominal variable by using a cutoff value of 10 mm, the SD of the largest LN was no longer a significant predictor in the decision tree model. Nevertheless, a larger LN raises suspicion of pathologic conditions such as malignancy, suggesting that the use of a cutoff diameter offers

limited effectiveness for differential diagnosis, and that it is important to consider other clinical and radiologic findings.

Although we used both clinical information and radiologic findings to establish the DTA models based on all predictors and categorical parameters, none of the clinical findings were identified as significant variables in the predictive models. US and US-guided biopsy were performed without serologic examinations in some patients; for example, only 78.1% of reactive hyperplasia patients underwent laboratory tests for the WBC count, and ESR measurements were performed with US in only 51.9%–75.6% of the patients in each disease group. If the laboratory tests had been performed in all patients, the results could have been different in that the WBC count, which showed statistically significant differences among the four disease groups, could be included as the predictor in the DTA model. In addition, although clinical findings and physical examination play important roles in primary management of pediatric cervical lymphadenopathy [43], the symptoms in cervical lymphadenopathy disease groups are often nonspecific [39], and interexaminer reliability for pediatric physical examinations has often been reported to be poor, moderate, and fair

in various diseases [44–46]. Therefore, radiologic evaluation of pediatric cervical lymphadenopathy would be useful for differential diagnosis and may improve diagnostic accuracy.

Our study had some limitations. This retrospective study had a limited study population. We excluded patients whose pathologic diagnosis was made only by fine needle aspiration (FNA) biopsy except in suppurative lymphadenitis and lymphoma, since FNA yields many inconclusive reports such as “nonspecific benign” or “inadequate.” Second, establishment and external validation of the diagnostic tree for pediatric cervical lymphadenopathy were made only with single tertiary hospital data. Third, Kikuchi disease is particularly prevalent in East Asia. Therefore, the decision tree is likely to show different diagnostic capacity in other regions, which may limit its applicability. Fourth, for excisional biopsy or CNB, one or two representative LNs was selected and pathologically identified. Therefore, there could be selection bias that Kikuchi disease or suppurative lymphadenitis may not be diagnosed in the reactive hyperplasia group. Fifth, in this study, evaluation of pediatric cervical lymphadenopathy with other modalities, such as CT and MRI, was not considered. Ultrasound is an excellent initial

imaging modality in pediatric cervical lymphadenopathy. Therefore, CT or MRI is rarely performed for initial diagnosis. However, there are several factors that can increase the discriminating ability of pediatric cervical lymphadenopathy, such as necrotic patterns of CT. Therefore, further research regarding US with the other modalities would be helpful in pediatric cervical lymphadenopathy. Finally, other cervical lymphadenopathies in children were not included in the diagnostic tree. Further studies including a large population of patients with various disease entities may be helpful in the differentiation of multiple pediatric cervical lymphadenopathies.

In conclusion, the presence of perinodal fat hyperechogenicity, heterogeneity of echotexture, and loss of fatty hilum were significant US findings in the DTA for differential diagnosis of cervical lymphadenopathy in children. However, the application of the SD cutoff of the largest LNs in the DTA model offers limited effectiveness due to the diversity of the population, and other clinical and radiological findings should be taken into account.

Reference

1 Park YW (1995) Evaluation of neck masses in children. Am Fam Physician 51:1904-1912

2 Bozlak S, Varkal MA, Yildiz I et al (2016) Cervical lymphadenopathies in children: A prospective clinical cohort study. International Journal of Pediatric Otorhinolaryngology 82:81-87

3 Deosthali A, Donches K, DelVecchio M, Aronoff S (2019) Etiologies of Pediatric Cervical Lymphadenopathy: A Systematic Review of 2687 Subjects. Global pediatric health 6:2333794X19865440-12333794X19865440

4 De Corti F, Cecchetto G, Vendraminelli R, Mognato G (2014) Fine-needle aspiration cytology in children with superficial lymphadenopathy. Pediatr Med Chir 36:80-82

5 Gwili N, Abdel-Hadi M, Nour-Eldin A et al (2014) Lymphadenopathy in a Series of Egyptian Pediatric Patients and the Role of Pathology in the Diagnostic Workup. Pediatr Dev Pathol. 10.2350/14-05-1480-oa.1

6 Sarsu SB, Sahin K (2016) A retrospective evaluation of lymphadenopathy in children in a single center's experience. J Pak Med Assoc 66:654-657

7 Lee EJ, Lee HS, Park JE, Hwang JS (2018) Association Kikuchi disease with Hashimoto thyroiditis: a case report and literature review. Annals of pediatric endocrinology & metabolism 23:99-102

8 Lee K-Y, Yeon Y-H, Lee B-C (2004) Kikuchi-Fujimoto Disease With Prolonged Fever in Children. Pediatrics 114:e752

9 Chiappini E, Camaioni A, Benazzo M et al (2015) Development of

an algorithm for the management of cervical lymphadenopathy in children: Consensus of the Italian Society of Preventive and Social Pediatrics, jointly with the Italian Society of Pediatric Infectious Diseases and the Italian Society of Pediatric Otorhinolaryngology. Expert review of anti-infective therapy 13:1-11

10 Aulino JM, Kirsch CFE, Burns J et al (2019) ACR Appropriateness Criteria((R)) Neck Mass-Adenopathy. J Am Coll Radiol 16:S150-s160

11 Ghafoori M, Azizian A, Pourrajabi Z, Vaseghi H (2015) Sonographic Evaluation of Cervical Lymphadenopathy; Comparison of Metastatic and Reactive Lymph Nodes in Patients With Head and Neck Squamous Cell Carcinoma Using Gray Scale and Doppler Techniques. Iran J Radiol 12:e11044

12 Nozaki T, Morita Y, Hasegawa D et al (2016) Cervical ultrasound and computed tomography of Kawasaki disease: Comparison with lymphadenitis. Pediatr Int 58:1146-1152

13 Ryoo I, Suh S, Lee YH, Seo HS, Seol HY (2015) Comparison of Ultrasonographic Findings of Biopsy-Proven Tuberculous Lymphadenitis and Kikuchi Disease. Korean J Radiol 16:767-775

14 Strassen U, Geisweid C, Hofauer B, Knopf A (2018) Sonographic differentiation between lymphatic and metastatic diseases in cervical lymphadenopathy. Laryngoscope 128:859-863

15 Dogan S, Yildirim A, Erbakirci R et al (2016) The Role of Ultrasonography for Differentiating and Management of Malignant Cervical Lymph Nodes. 13:7-15

16 Ahuja AT, Ying M (2005) Sonographic evaluation of cervical lymph nodes. AJR Am J Roentgenol 184:1691-1699

17 Khanna R, Sharma AD, Khanna S, Kumar M, Shukla RC (2011)

Usefulness of ultrasonography for the evaluation of cervical lymphadenopathy. World journal of surgical oncology 9:29−29

18 You SH, Kim B, Yang KS, Kim BK (2019) Cervical necrotic lymphadenopathy: a diagnostic tree analysis model based on CT and clinical findings. Eur Radiol 29:5635−5645

19 Baek HJ, Lee JH, Lim HK, Lee HY, Baek JH (2014) Diagnostic accuracy of the clinical and CT findings for differentiating Kikuchi's disease and tuberculous lymphadenitis presenting with cervical lymphadenopathy. Jpn J Radiol 32:637−643

20 Kwon SY, Kim TK, Kim YS, Lee KY, Lee NJ, Seol HY (2004) CT findings in Kikuchi disease: analysis of 96 cases. AJNR Am J Neuroradiol 25:1099−1102

21 Lee S, Yoo JH, Lee SW (2012) Kikuchi Disease: Differentiation from Tuberculous Lymphadenitis Based on Patterns of Nodal Necrosis on CT. American Journal of Neuroradiology 33:135

22 Kim JY, Lee H, Yun BL (2017) Ultrasonographic findings of Kikuchi cervical lymphadenopathy in children. Ultrasonography (Seoul, Korea) 36:66−70

23 Lee MH, Lee SW, Kang BC (1999) Ultrasonographic Evaluation of Suppurative Cervical Lymphadenitis in Children : Focusing on Abscess Formation. Ultrasonography (Seoul, Korea) 18:313−318

24 Lo WC, Chang WC, Lin YC, Hsu YP, Liao LJ (2012) Ultrasonographic differentiation between Kikuchi's disease and lymphoma in patients with cervical lymphadenopathy. Eur J Radiol 81:1817−1820

25 Onciu M, Medeiros LJ (2003) Kikuchi−Fujimoto lymphadenitis. Adv Anat Pathol 10:204−211

26 Yoo JL, Suh SI, Lee YH et al (2011) Gray scale and power Doppler study of biopsy-proven Kikuchi disease. J Ultrasound Med 30:957-963

27 Marcy SM (1985) Cervical adenitis. Pediatr Infect Dis 4:S23-26

28 Schwetschenau E, Kelley DJ (2002) The adult neck mass. Am Fam Physician 66:831-838

29 Hernandez M, Chowdhury R, Woods J, Cabrera J, Hardigan PC (2011) Management of suppurative cervical lymphadenitis in a healthy 24-year-old man. J Am Osteopath Assoc 111:49-51

30 Kikuchi M (1972) Lymphadenitis showing focal reticulum cell hyperplasia with nuclear debris and phagocytes : a clinicopathological study. Acta Haematol Jpn 35:379-380

31 Kuo TT (1995) Kikuchi's disease (histiocytic necrotizing lymphadenitis). A clinicopathologic study of 79 cases with an analysis of histologic subtypes, immunohistology, and DNA ploidy. Am J Surg Pathol 19:798-809

32 Perry AM, Choi SM (2018) Kikuchi-Fujimoto Disease: A Review. Archives of Pathology & Laboratory Medicine 142:1341-1346

33 Ahuja A, Ying M, Yang WT, Evans R, King W, Metreweli C (1996) The use of sonography in differentiating cervical lymphomatous lymph nodes from cervical metastatic lymph nodes. Clin Radiol 51:186-190

34 Ishii J, Fujii E, Suzuki H, Shinozuka K, Kawase N, Amagasa T (1992) Ultrasonic diagnosis of oral and neck malignant lymphoma. Bull Tokyo Med Dent Univ 39:63-69

35 Bruneton JN, Normand F, Balu-Maestro C et al (1987) Lymphomatous superficial lymph nodes: US detection. Radiology

165:233-235

36 Ying M, Ahuja A, Brook F, Brown B, Metreweli C (1996) Sonographic appearance and distribution of normal cervical lymph nodes in a Chinese population. J Ultrasound Med 15:431-436

37 Leboulleux S, Girard E, Rose M et al (2007) Ultrasound criteria of malignancy for cervical lymph nodes in patients followed up for differentiated thyroid cancer. J Clin Endocrinol Metab 92:3590-3594

38 Ganeshalingam S, Koh DM (2009) Nodal staging. Cancer Imaging 9:104-111

39 Ferrer R (1998) Lymphadenopathy: differential diagnosis and evaluation. Am Fam Physician 58:1313-1320

40 Libman H (1987) Generalized lymphadenopathy. J Gen Intern Med 2:48-58

41 Morland B (1995) Lymphadenopathy. Arch Dis Child 73:476-479

42 Slap GB, Brooks JS, Schwartz JS (1984) When to perform biopsies of enlarged peripheral lymph nodes in young patients. Jama 252:1321-1326

43 Citak EC, Koku N, Demirci M, Tanyeri B, Deniz H (2011) A retrospective chart review of evaluation of the cervical lymphadenopathies in children. Auris Nasus Larynx 38:618-621

44 Giovanni JE, Dowd MD, Kennedy C, Michael JG (2011) Interexaminer agreement in physical examination for children with suspected soft tissue abscesses. Pediatr Emerg Care 27:475-478

45 Yen K, Karpas A, Pinkerton HJ, Gorelick MH (2005) Interexaminer reliability in physical examination of pediatric patients with abdominal pain. Arch Pediatr Adolesc Med 159:373-376

46 Marin JR, Bilker W, Lautenbach E, Alpern ER (2010) Reliability of clinical examinations for pediatric skin and soft-tissue infections. Pediatrics 126:925-930

Table 1. Comparison of Clinical Characteristics for Kikuchi Disease, Reactive Hyperplasia, Lymphoma, and Suppurative Lymphadenitis

Diagnosis	Kikuchi disease (n=127)	Reactive hyperplasia (n=64)	Lymphoma (n=24)	Suppurative lymphadenitis (n=27)	Total (N=242)
Sex					
Male	67 (52.8%)	35 (54.7%)	20 (83.3%)	9 (33.3%)	131 (54.1%)
Female	60 (47.2%)	29 (45.3%)	4 (16.7%)	18 (66.7%)	111 (45.9%)
Age	12.11 ± 0.30	11.86 ± 0.62	12.42 ± 0.94	4.04 ± 0.90	11.17 ± 0.31
LN tenderness					
Positive	65 (51.2%)	17 (26.6%)	4 (16.7%)	21 (77.8%)	107 (44.2%)
Negative	62 (48.8%)	47 (73.4%)	20 (83.3%)	6 (22.2%)	135 (55.8%)
LN erythema					
Positive	1 (0.8%)	2 (3.1%)	0 (0.0%)	11 (40.7%)	30 (5.8%)
Negative	126 (99.2%)	62 (96.9%)	24 (100.0%)	16 (59.3%)	14 (94.2%)
LN heat sense					
Positive	8 (6.3%)	1 (1.6%)	0 (0.0%)	7 (25.9%)	16 (6.6%)
Negative	119 (93.7%)	63 (98.4%)	24 (100.0%)	20 (74.1%)	226 (93.4%)
Fever					
Positive	93 (73.2%)	27 (42.2%)	6 (25.0%)	19 (70.4%)	145 (59.9%)
Negative	34 (26.8%)	37 (57.8%)	18 (75.0%)	8 (29.6%)	97 (40.1%)
Prolonged fever					
Positive	35 (27.6%)	9 (14.1%)	1 (4.2%)	2 (7.4%)	47 (19.4%)
Negative	92 (72.4%)	55 (85.9%)	23 (95.8%)	25 (92.6%)	195 (80.6%)
Hepatomegaly					
Positive	1 (0.8%)	0 (0.0%)	2 (8.3%)	0 (0.0%)	3 (1.2%)
Negative	126 (99.2%)	64 (100.0%)	22 (91.7%)	27 (100.0%)	239 (98.8%)
Splenomegaly					
Positive	4 (3.1%)	0 (0.0%)	1 (4.2%)	0 (0.0%)	5 (2.1%)
Negative	123	64 (100.0%)	23 (95.8%)	27 (100.0%)	237

	(96.9%)				(97.9%)
Use of antibiotics					
Positive	72 (57.1%)	19 (29.7%)	6 (25.0%)	15 (55.6%)	111 (46.3%)
Negative	54 (42.9%)	45 (70.3%)	18 (75.0%)	12 (44.4%)	129 (53.8%)
Pathologic diagnosis					
FNA	0 (0.0%)	0 (0.0%)	0 (0.0%)	15 (55.6%)	15 (6.2%)
CNB	125 (98.4%)	58 (90.6%)	5 (20.8%)	7 (25.9%)	195 (80.6%)
Excision	2 (1.6%)	6 (9.4%)	19 (79.2%)	5 (18.5%)	32 (13.2%)
WBC count (10^3)	3.80 ± 1.55 (n = 118)	7.41 ± 4.01 (n = 50)	9.05 ± 4.56 (n = 24)	16.57 ± 7.93 (n = 27)	6.78 ± 5.65 (n = 219)
WBC count range					
Leukopenia	73 (61.9%)	8 (16.0%)	1 (4.1%)	0 (0.0%)	82 (37.4%)
Normal range	45 (38.1%)	35 (70.0%)	19 (79.2%)	10 (37.0%)	109 (49.8%)
Leukocytosis	0 (0.0%)	7 (14.0%)	4 (16.7%)	17 (63.0%)	28 (12.8%)
ESR	30.25 ± 20.27 (n = 96)	20.95 ± 20.92 (n = 40)	15.50 ± 16.73 (n = 14)	40.21 ± 31.05 (n = 14)	27.57± 22.01 (n = 164)
CRP	1.27 ± 1.91 (n = 107)	1.16 ± 2.76 (n = 43)	2.87 ± 5.69 (n = 24)	3.52 ± 3.46 (n = 27)	1.74 ± 3.10 (n = 201)

Data are mean ± standard deviation (SD) for continuous variables and the number of patients (%) for nominal variables.

WBC, white blood cell count; ESR, erythrocyte sedimentation rate; CRP, c-reactive protein; FNA, fine needle aspiration; CNB, core needle biopsy

Table 2. Comparison of Neck US Imaging Findings for Kikuchi Disease, Reactive Hyperplasia, Lymphoma, and Suppurative Lymphadenitis

Diagnosis	Kikuchi disease (n=127)	Reactive hyperplasia (n=64)	Lymphoma (n=24)	Suppurative lymphadenitis (n=27)	Total (N=242)
Laterality					
Unilateral	95 (74.8%)	32 (50.0%)	12 (50.0%)	26 (96.3%)	165 (68.2%)
Bilateral	32 (25.2%)	32 (50.0%)	12 (50.0%)	1 (3.7%)	77 (31.8%)
Posterior Neck Involvement					
Positive	93 (73.2%)	37 (57.8%)	10 (41.7%)	2 (7.4%)	142 (58.7%)
Negative	34 (26.8%)	27 (42.2%)	14 (58.3%)	25 (92.6%)	100 (41.3%)
LN Number					
Single (1)	4 (3.1%)	5 (7.8%)	7 (29.2%)	10 (37.0%)	26 (10.7%)
Several (2-4)	7 (5.5%)	14 (21.9%)	2 (8.3%)	9 (33.3%)	32 (13.2%)
Multiple (≥5)	116 (91.3%)	45 (70.3%)	15 (62.5%)	8 (29.6%)	184 (76.0%)
LN Distribution					
Conglomerated	114 (89.8%)	26 (40.6%)	14 (58.3%)	16 (59.3%)	170 (70.2%)
Separated	13 (10.2%)	38 (59.4%)	10 (41.7%)	11 (40.7%)	72 (29.8%)
LN Size Distribution					
Even	106 (83.5%)	19 (29.7%)	2 (8.3%)	1 (3.7%)	128 (52.9%)
Uneven	21 (16.5%)	45 (70.3%)	22 (91.7%)	26 (96.3%)	114 (47.1%)
Short (mm)	18.27 ± 5.44	19.18 ± 5.75	29.49 ± 13.82	27.00 ± 8.38	20.60 ± 8.11
Short diameter (mm)	8.56 ± 2.95	8.28 ± 3.22	17.27 ±7.64	18.43 ±6.00	10.45 ±5.62
SD < 10mm	97 (76.4%)	45 (70.3%)	3 (12.5%)	3 (11.1%)	148 (61.2%)
SD ≥ 10mm	30 (23.6%)	19 (29.7%)	21 (87.5%)	24 (88.9%)	94 (38.8%)
Shape of LN (SD/LD ratio)	0.48 ± 0.11	0.43 ± 0.12	0.60 ± 0.11	0.70 ±0.15	0.50 ± 0.14
Elongated (< 0.5)	78	47 (73.4%)	5 (20.8%)	3 (11.1%)	133

	(61.4%)				(55.0%)
Oval (0.5–0.7)	45 (35.4%)	15 (23.4%)	15 (62.5%)	10 (37.0%)	85 (35.1%)
Round (> 0.7)	4 (3.1%)	2 (3.1%)	4 (16.7%)	14 (51.9%)	24
Echogenicity of LN compared with muscle					
Hypoechoic	123 (96.9%)	62 (96.9%)	22 (91.7%)	22 (81.5%)	229 (94.6%)
Isoechoic and Hyperechoic	4 (3.1%)	2 (3.1%)	2 (8.3%)	5 (18.5%)	13 (5.4%)
LN Heterogenicity					
Homogeneous	127 (100.0%)	59 (92.2%)	14 (58.3%)	1 (3.7%)	201 (83.1%)
Heterogeneous	0 (0.0%)	5 (7.8%)	10 (41.7%)	26 (96.3%)	41 (16.9%)
LN Margin					
Well–defined	126 (99.2%)	63 (98.4%)	20 (83.3%)	4 (14.8%)	213 (88.0%)
Ill–defined	1 (0.8%)	1 (1.6%)	4 (16.7%)	23 (85.2%)	29 (12.0%)
LN Necrosis/Abscess					
Positive	0 (0.0%)	0 (0.0%)	1 (4.2%)	23 (85.2%)	24 (9.9%)
Negative	127 (100.0%)	64 (100.0%)	23 (95.8%)	4 (14.8%)	218 (90.1%)
LN Calcification					
Positive	0 (0.0%)	0 (0.0%)	0 (0.0%)	0 (0.0%)	0 (0.0%)
Negative	127 (100.0%)	64 (100.0%)	24 (100.0%)	27 (100.0%)	242 (100.0%)
Loss of Fatty Hilum					
Positive	1 (0.8%)	2 (3.1%)	17 (70.8%)	24 (88.9%)	44 (18.2%)
Negative	126 (99.2%)	62 (96.9%)	7 (29.2%)	3 (11.1%)	198 (81.8%)
LN Hilar vascularity	(n = 103)	(n = 49)	(n = 21)	(n = 22)	(n = 195)
Normal	102 (99.0%)	46 (93.9%)	7 (33.3%)	3 (13.6%)	158 (81.0%)
Abnormal	1 (1.0%)	3 (6.1%)	14 (66.7%)	19 (86.4%)	37 (19.0%)
Perinodal/Cortical Vascularity	(n = 103)	(n = 49)	(n = 21)	(n = 22)	(n = 195)
Positive	45 (43.7%)	4 (8.2%)	4 (19.0%)	19 (86.4%)	72 (36.9%)
Negative	58 (56.3%)	45 (91.8%)	17 (81.0%)	3 (13.6%)	123 (63.1%)
Perinodal Fat Hyperechogenicity					

Positive	117 (92.1%)	14 (21.9%)	4 (16.7%)	26 (96.3%)	161 (66.5%)
Negative	10 (7.9%)	50 (78.1%)	20 (83.3%)	1 (3.7%)	81 (33.5%)
Perinodal Fluid dispersion					
Positive	13 (10.2%)	0 (0.0%)	3 (12.5%)	4 (14.8%)	20 (8.3%)
Negative	114 (89.8%)	64 (100.0%)	21 (87.5%)	23 (85.2%)	222 (91.7%)

Data are mean ± standard deviation (SD) for continuous variables and the number of patients (%) for nominal variables

LN, lymph node

Table 3. Performance of the Diagnostic Trees

			Prediction					
		Diagnosis	Kikuchi's disease	Reactive hyperplasia	Lymphoma	Suppurative lymphadenitis	Accuracy (%)	Balanced Accuracy (%)
All predictors	Training Data set	Kikuchi's disease (n = 89)	83	6	0	0	93.3	88.6
		Reactive hyperplasia (n = 45)	10	35	0	0	77.8	84.9
		Lymphoma (n = 17)	2	4	10	1	58.9	79.1
		Suppurative lymphadenitis (n = 19)	1	0	1	17	89.5	94.4
		Overall (n = 170)					85.3	
	External validation data set	Kikuchi's disease (n = 38)	34	3	1	0	89.5	88.9
		Reactive hyperplasia (n = 19)	3	15	0	1	78.9	82.8
		Lymphoma (n = 7)	1	3	3	0	42.9	70.7
		Suppurative lymphadenitis (n = 8)	0	0	0	8	100.0	99.2
		Overall (n = 72)					83.3	
Categorical predictors	Training data set	Kikuchi's disease (n = 89)	83	5	1	0	93.3	88.6
		Reactive hyperplasia (n = 45)	10	33	2	0	73.3	83.1
		Lymphoma (n = 17)	2	3	11	1	64.7	81.4
		Suppurative lymphadenitis (n = 19)	1	1	0	17	89.5	94.4
		Overall (n = 170)					84.7	
	External validation data set	Kikuchi's disease (n = 38)	34	4	0	0	89.5	88.9
		Reactive hyperplasia (n = 19)	3	15	0	1	78.9	84.8
		Lymphoma (n = 7)	1	1	5	0	71.4	85.7
		Suppurative lymphadenitis (n = 8)	0	0	0	8	100.0	99.2
		Overall (n = 72)					86.1	

Figure 1. Flow chart for patient inclusion and exclusion

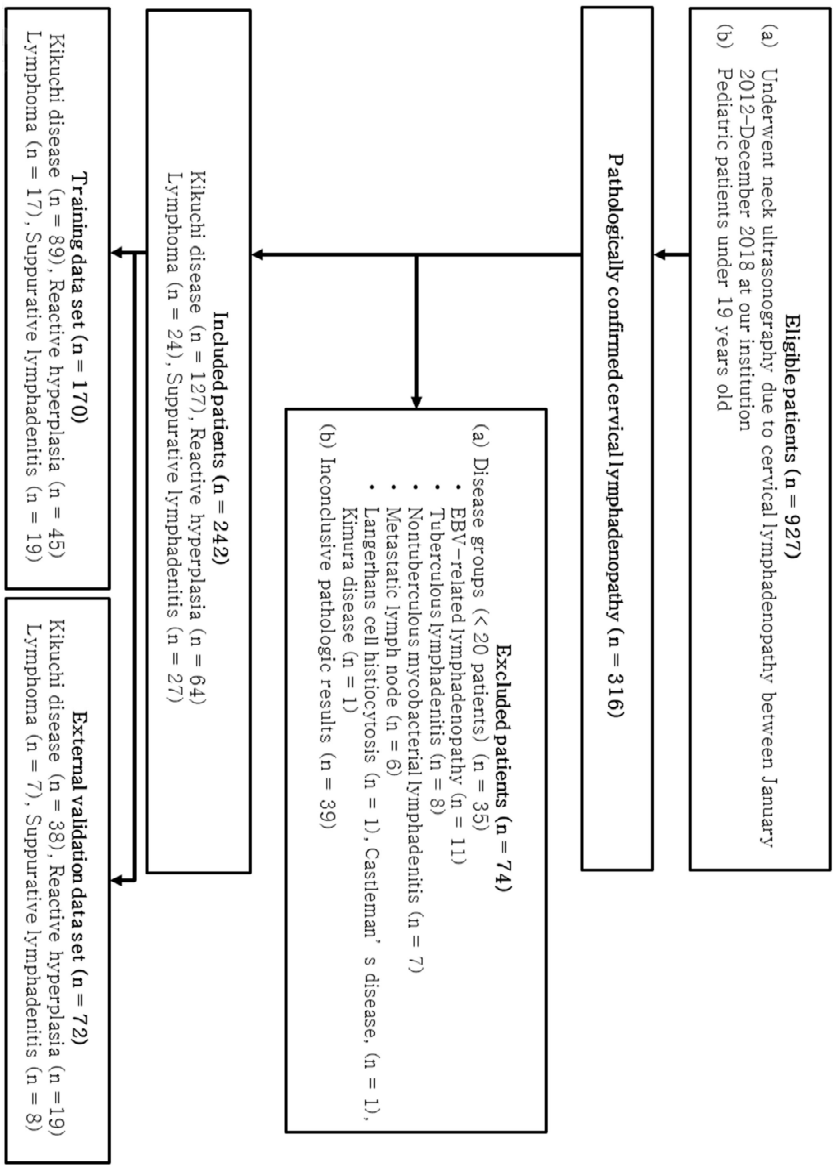

Figure 2. Representative ultrasonographic images in patients with Kikuchi's disease, reactive hyperplasia, lymphoma, and suppurative lymphadenitis

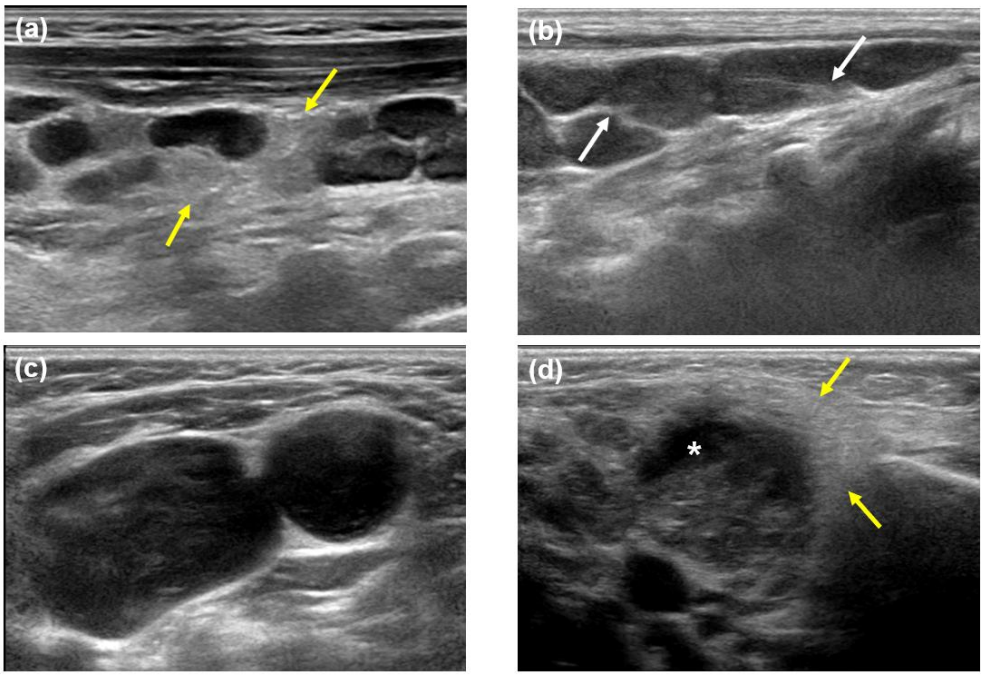

(a) 12-year-old boy with Kikuchi disease, cervical lymph node shows homogeneous hypoechoic texture with increased perinodal echogenicity (yellow arrows).

(b) 6-year-old boy with reactive hyperplasia, elongated hypoechoic cortex with echogenic hilum (white arrows)

(c) 11-year-old boy with lymphoma, markedly enlarged hypoechoic lymph node is in the left level III with loss of fatty hilum. There is no evidence of perinodal fat infiltration

(d) 7-month-old girl with suppurative lymphadenitis, US image demonstrates heterogeneous cervical lymph node with central abscess (asterisk) and perinodal fat hyperechogenicity (yellow arrows).

Figure 3. Diagnostic tree derived from all predictors of imaging findings and clinical information

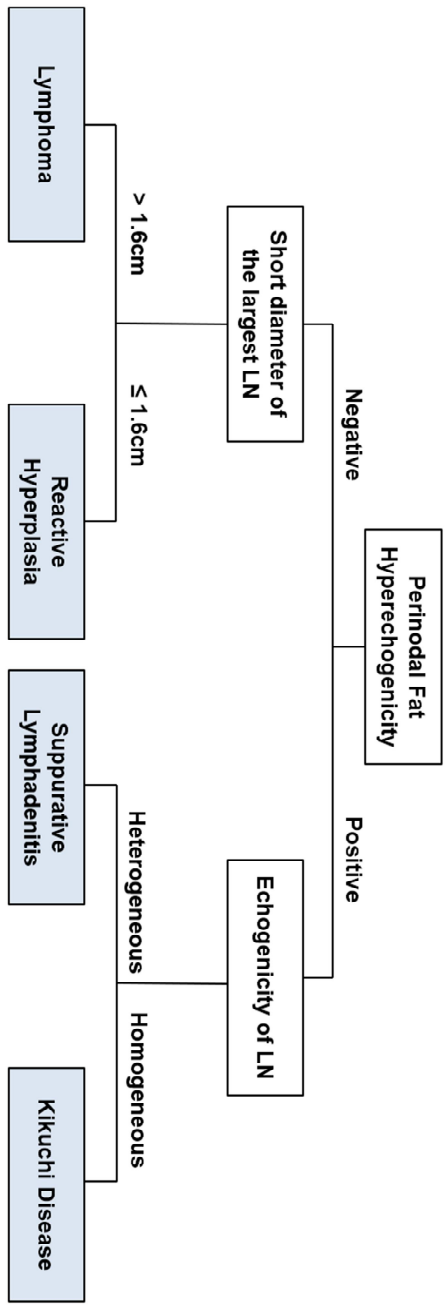

Figure 4. Diagnostic tree derived from categorical predictors of imaging findings and clinical information

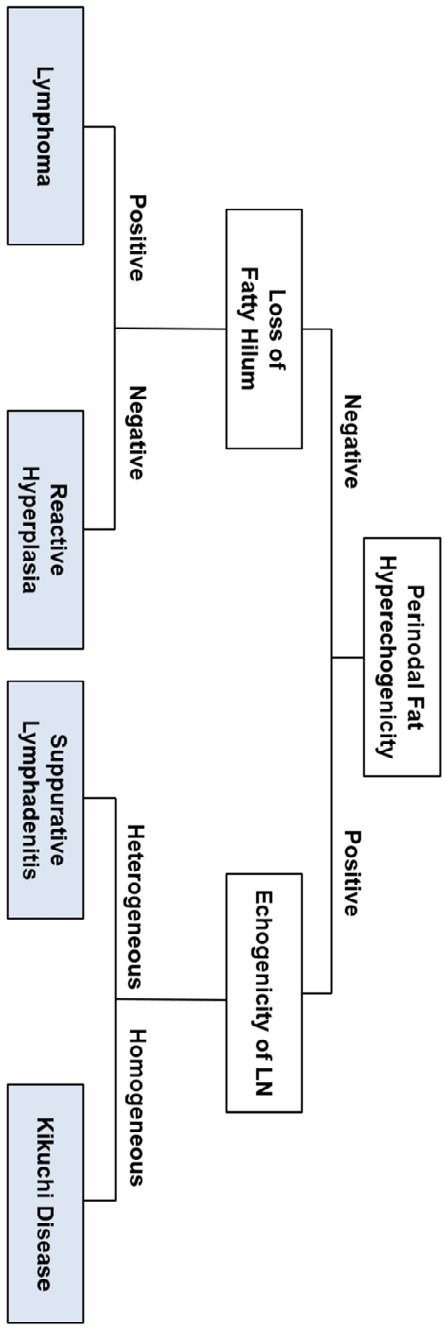

논 문 초 록

목적: 소아의 경부 림프절 비대를 감별하는데 도움을 줄 수 있는 진단나무모형을 초음파와 임상 소견에 근거하여 만들고자 한다.

대상 및 방법: 2012 년 1 월부터 2018 년 12 월까지 경부 림프절 초음파를 시행하고, 침 생검 혹은 수술적 생검을 시행 받은 18 세 이하 환자 중 반응성 림프절 증식, 화농성 림프절염, 키쿠치병, 림프종으로 확진 된 18 세 이하 환자, 총 242 명의 (131 명의 남아, 111 명의 여아, 평균 나이 11.2 ± 0.3 세, 연령 범위 1 개월-18 세)이 연구대상으로 포함되었다.

진단 당시의 의무기록을 후향적으로 분석하여 연령, 성별, 경부 압통/열감/홍반, 발열, 간비대, 비비대, 항생제 복용 여부, 혈액학적 검사결과 (백혈구 수, CRP, ESR)를 확인하였다.'

병리적인 진단 2 주내에 시행된 초음파 영상을 두명의 영상의학과 의사가 후향적으로 분석하여 비대 된 림프절 위치, 개수, 분포, 크기, 에코 정도 및 균질성, 경계, 괴사의 여부, 석회화의 여부, 림프절 주변 지방 에코 증가, 정상적인 림프절 문 (fatty hilum)의 소실 여부, 색조 도플러 영상 소견 등을 평가하였다.

이로부터 얻어진 임상, 영상소견을 분류회귀나무 (classification and regression tree, CART) 알고리즘을 이용해 진단나무모형을 개발했다. 총 데이터를 무작위로 분류하여 70%는 훈련 데이터로, 나머지 30%는 검증 데이터로 분석하여 진단나무모형의 진단력을 평가하였다.

결과: 모든 예측 인자에 기초한 진단나무모형에서 림프절 주변 고에코, 림프절 내부 에코의 균일성 및 가장 큰 림프절의 짧은 직경은 경부 림프절 병증의 감별 진단을 위한 진단 알고리즘에서 유의한 예측 인자였다. 훈련 데이터세트에서 진단나무모형의 진단 정확도는 85.3%, 검증 데이터 세트에서의 정확도는 83.3% 였다.

범주형 변수만을 이용한 DTA 모델에서는 림프절 주변 고에코, 림프절 내부 에코의 균일성, 림프절 지방문의 소실이 진단에 중요한 예측 인자였으며 훈련 데이터세트에서 진단나무모형의 진단 정확도는 84.7%, 검증 데이터 세트에서는 86.1%를 보였다.

결론: 소아의 경부 림프절 비대를 감별 진단하기 위해 초음파 소견 및 임상 소견에 근거하여 만든 진단나무모형에서 림프절 주변 고에코, 림프절 내부 에코의 균일성, 가장 큰 림프절의 짧은 직경, 림프절 지방문의 소실이 유의한 결정 인자였다. 그러나 가장 큰 림프절의 짧은 직경은 우리 연구 이외의 환자군에서 적용하는데 제한이 있으므로 환자의 임상 소견 및 다른 초음파 소견도 함께 고려하여야 한다.

주요어: 림프절 비대, 초음파, 진단 나무, 키쿠치병, 림프종

학번: 2018-24517